

Article

3D Virtual Modeling for Morphological Characterization of Pituitary Tumors: Preliminary Results on Its Predictive Role in Tumor Resection Rate

Laura Cercenelli ^{1,*}, Matteo Zoli ^{2,3,†}, Barbara Bortolani ¹, Nico Curti ¹, Davide Gori ³, Arianna Rustici ^{4,5}, Diego Mazzatenta ^{2,3} and Emanuela Marcelli ¹

¹ eDIMES Lab–Laboratory of Bioengineering, Department of Experimental, Diagnostic and Specialty Medicine (DIMES), University of Bologna, 40138 Bologna, Italy; barbara.bortolani@unibo.it (B.B.); nico.curti@unibo.it (N.C.); emanuela.marcelli@unibo.it (E.M.)

² Pituitary Unit, Center for Diagnosis and Treatment of Hypothalamic-Pituitary Diseases, 40139 Bologna, Italy; matteo.zoli4@unibo.it (M.Z.); diego.mazzatenta@unibo.it (D.M.)

³ Department of Biomedical and Motor Sciences (DIBINEM), University of Bologna, 40138 Bologna, Italy; davide.gori4@unibo.it

⁴ Department of Neuroradiology, IRCCS Institute of Neurological Sciences of Bologna, 40139 Bologna, Italy; arianna.rustici2@unibo.it

⁵ Department of Experimental, Diagnostic and Specialty Medicine (DIMES), University of Bologna, 40138 Bologna, Italy

* Correspondence: laura.cercenelli@unibo.it

† These authors contributed equally to this work.



Citation: Cercenelli, L.; Zoli, M.; Bortolani, B.; Curti, N.; Gori, D.; Rustici, A.; Mazzatenta, D.; Marcelli, E. 3D Virtual Modeling for Morphological Characterization of Pituitary Tumors: Preliminary Results on Its Predictive Role in Tumor Resection Rate. *Appl. Sci.* **2022**, *12*, 4275. <https://doi.org/10.3390/app12094275>

Academic Editors: Manuel Duarte Ortigueira, Carla M. A. Pinto, Arnaldo Guimarães Batista, Álvaro Astasio Picado and Jia Chen

Received: 19 February 2022

Accepted: 21 April 2022

Published: 23 April 2022

Publisher's Note: MDPI stays neutral with regard to jurisdictional claims in published maps and institutional affiliations.

Abstract: Among potential factors affecting the surgical resection in pituitary tumors, the role of tumor three-dimensional (3D) features is still unexplored. The aim of this study is to introduce the use of 3D virtual modeling for geometrical and morphological characterization of pituitary tumors and to evaluate its role as a predictor of total tumor removal. A total of 75 patients operated for a pituitary tumor have been retrospectively reviewed. Starting from patient imaging, a 3D tumor model was reconstructed, and 3D characterization based on tumor volume (Vol), area, sphericity (Spher), and convexity (Conv) was provided. The extent of tumor removal was then evaluated at post-operative imaging. Mean values were obtained for Vol ($9117 \pm 8423 \text{ mm}^3$), area ($2352 \pm 1571 \text{ mm}^2$), Spher (0.86 ± 0.08), and Conv (0.88 ± 0.08). Total tumor removal was achieved in 57 (75%) cases. The standard prognostic Knosp grade, Vol, and Conv were found to be independent factors, significantly predicting the extent of tumor removal. Total tumor resection correlated with lower Knosp grades ($p = 0.032$) and smaller Vol ($p = 0.015$). Conversely, tumors with a more irregular shape (low Conv) have an increased chance of incomplete tumor removal ($p = 0.022$). 3D geometrical and morphological features represent significant independent prognostic factors for pituitary tumor resection, and they should be considered in pre-operative planning to allow a more accurate decision-making process.

Keywords: pituitary tumors; 3D virtual modeling; outcome predictors; 3D morphological features; biomedical image processing



Copyright: © 2022 by the authors. Licensee MDPI, Basel, Switzerland. This article is an open access article distributed under the terms and conditions of the Creative Commons Attribution (CC BY) license (<https://creativecommons.org/licenses/by/4.0/>).

1. Introduction

The ideal target of surgery for pituitary tumors is represented by their complete removal [1,2]. However, this aim cannot be achieved in a consistent rate of adenomas, for their location in the depth of the skull base and their close proximity to multiple relevant anatomical structures, such as carotid arteries, optic nerves, cavernous sinuses, and diencephalon [1,3–7]. Indeed, despite the recent implementation of modern technological devices for transsphenoidal surgery, such as neuro-navigation, intra-operative doppler, dedicated echographic probes, intra-operative computed tomography (CT) or magnetic resonance imaging (MRI), or three-dimensional endoscopes, the finding of tumor remnants

at post-operative neuroimaging remains an open issue [1,3–7]. These neoplastic residuals may require a close follow-up, especially for peculiar histotypes, which have been demonstrated to be at higher risk of progression (i.e., sparsely granulated somatotroph, lactotroph, Crooke's cell, silent corticotroph, or plurihormonal Pit-1-positive tumors), or for tumors with higher Trouillas grades, such as 1B or 2B, according to a recently proposed score [8–11]. Moreover, the incomplete tumor resection would lead to a lack of control of hormonal hyper-secretion, requiring adjunctive therapies such as specific endocrinological medications, radiation treatments, or second surgeries, or to the possible partial or full persistence of compressive symptoms [12,13].

Many studies have focused on the possibility to pre-operatively predict the risk of incomplete tumor resection, in order to improve the pre-surgical planning and the overall treatment strategy and to guide the patient's counseling [14–19]. One of the more relevant prognostic factors has been found to be the cavernous sinus (CS) invasion, expressed by the Knosp grade [14–19]. Indeed, the removal of adenomas extends into this peculiar anatomical structure, which contains cranial nerves (CNs), the internal carotid artery (ICA), and which receives the venous drainage from a large portion of the skull base, is often impaired [14–19]. Moreover, the extensive infiltration of the bone or dural structures, the large or gigantic size of the adenoma, previous surgeries or radiotherapies, and fibrous consistency are reported as other negative prognostic factors for tumor resection [9,14,18,20–24].

Among these studies, few have focused on the possible predictive role of three-dimensional (3D) geometry and morphology of the tumor [14–22,24]. In particular, they have not investigated if any 3D morphological feature could be associated with a higher risk of incomplete tumor removal, limiting to qualitative investigations [14–22,24].

In the last decades, new tools based on 3D imaging and advanced digital technologies have become available to surgeons during pre-operative phases, and many experiences have been reported in the field of surgical oncology, including maxillofacial surgery [25,26], urology [27–29], and also neurosurgery [30]. In a recent study, the usefulness of a prognostic model based on the quantitative 3D characterization of tumor size and shape in patients with oral cavity squamous cell carcinoma has been demonstrated [31]. Based on this previous experience, the present study aims to investigate whether a 3D analysis of tumor shape may have an independent prognostic role to pre-operatively predict the extent of tumor resection and to identify which 3D feature of the tumor could be more significantly associated with a favorable surgical outcome.

2. Materials and Methods

2.1. Study Design

A total of 75 patients were selected for the subsequent study (41 male and 34 female). All patients operated on through an endoscopic endonasal approach (EEA) since 2008 and 2018 for a pituitary tumor at our Institution have been retrospectively investigated. Inclusion criteria were a size larger than 10 mm (macroadenomas), and availability of pre-/post-operative clinical data and MRI with/without gadolinium. In order to collect a homogenous series of cases, MRI scans with slice thickness greater than 1.0 mm or spacing between slices greater than 1.0 mm were excluded from the study.

Each patient had pre-operatively undergone a complete endocrinological status assessment, including serum LH, FSH, TSH, fT4, ACTH, cortisol, PRL, GH, and IGF-1 levels evaluation, as well as serum and urinary electrolytes and osmolarity. In the case of a clinical and bio-humoral suspect of hyper-secretion, specific tests were performed to confirm the diagnosis. An ophthalmological evaluation with computerized visual field analysis was performed for all patients, as well as a complete neurological examination. At pre-operative MRI, the Hardy–Wilson and Knosp grades, which are two commonly used grading systems based on the evaluation of planar (2D) diagnostic images, were considered [18]. The Zurich score, a recent score proposed by Serra et al., was retrospectively obtained, calculating

the ratio between the maximum horizontal diameter (HD) of the tumor and the minimal inter-carotid distance (ICD) at the horizontal segment [23].

The 3D geometrical and morphological features of the tumor (volume, area, sphericity, and convexity, respectively) were evaluated on pre-operative MRI, as described in the following paragraphs.

All patients were operated on by the same team of neurosurgeons and ENT surgeons in a tertiary referral center [1,32,33]. In all cases, a midline endoscopic endonasal approach was adopted following the surgical approach previously described [34]. Surgical complications were evaluated based on medical records.

Each patient had MRI with gadolinium performed 3 months after surgery to assess the extent of tumor removal. Resection was considered “total” in case of no remnant at MRI, “subtotal” if the volume of the remnant was inferior to 20% of the initial mass, “partial” if it included between 20% and 50%, and “incomplete” if larger than 50%. At the same follow-up, the endocrinological, visual, and neurological functions were reassessed, repeating the pre-operative tests.

The study was approved by an inter-hospital Ethical Committee of Bologna City (protocol #CE17143, February 2018).

2.2. 3D Characterization of Tumor

In order to provide a 3D characterization of the tumor, the pre-operative MRI images (DICOM data) of the study population were uploaded into D2P™ software (3D Systems Inc., Rock Hill, SC, USA), a modular software package designed to convert patients’ medical images into 3D digital models, that we extensively used in previous studies to introduce new volumetric virtual planning methods in the field of maxillofacial surgery and urological surgery [35–39].

Starting from the obtained 3D models of the anatomic regions of interest, the following indexes were calculated. All calculations were performed in MATLAB R2019a (The MathWorks, Natick, MA, USA).

2.3. Tumor Volume and Area

Multi-slice interpolation and threshold segmentation tools were used to segment the volumetric tumor extension, which was then converted to a 3D mesh and exported in STL format. For each 3D mesh of the segmented tumor mass, the corresponding volume (Vol) and surface area (Area) were calculated (Figure 1).

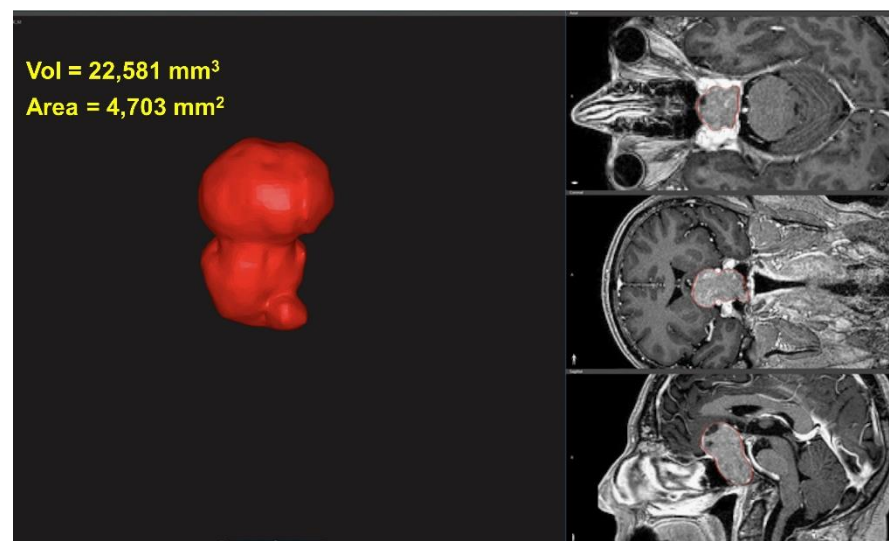


Figure 1. Example of segmented pituitary gland tumor obtained using D2P™ software, from MR scan. Vol = tumor volume; Area = tumor area.

2.4. Tumor Sphericity

Defined by Wadell in 1935 [40], the sphericity is a geometric measurement of how closely the shape of an object approaches that of a mathematically perfect sphere: the sphericity of a particle (p) is the ratio of the surface area of a sphere (with the same volume as the given particle) to the surface area of the particle (see Equation (1)).

$$S = \frac{\pi^{\frac{1}{3}}(6V_p)^{\frac{2}{3}}}{A_p} \tag{1}$$

where V_p is the volume of the particle (p) and A_p is the surface area of the particle. The sphericity of a sphere is equal to 1, so any particle that is not a sphere will have sphericity less than 1. We applied the sphericity measurement to the segmented tumor mass in order to obtain the tumor sphericity (Spher) index. Examples of Spher calculated for two different pituitary gland tumor masses are shown in Figure 2.

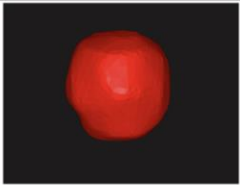
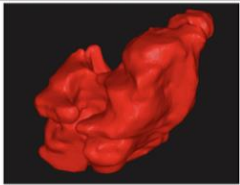
Case	017	015
Segmented pituitary gland tumor		
Spher	0.97	0.57

Figure 2. Examples of pituitary gland tumor with different sphericity (Spher) values: from high (left side) to low (right side) values.

2.5. Tumor Convexity

The tumor convexity (Conv) index is the ratio between the tumor volume and the convex hull volume. The convex hull of a set X of points in the Euclidean plane or in a Euclidean space is the smallest convex set that contains X [41]. In this specific case, the convex hull of a tumor is the smallest volume that fully encloses the tumor volume and that is convex at all points. The Conv index captures the degree of tumor surface regularity, and therefore it decreases for shapes with many irregularities, such as hollows and indentations.

For the 3D mesh of each tumor, we generated the tumor convex hull using the MATLAB function “convhull”. Then, we calculated the volumes of the tumor and the Conv index, as in Equation (2):

$$Conv = \frac{Volume}{ConvexHullVolume} \tag{2}$$

Examples of the Conv index calculated for two different pituitary gland tumors are shown in Figure 3.

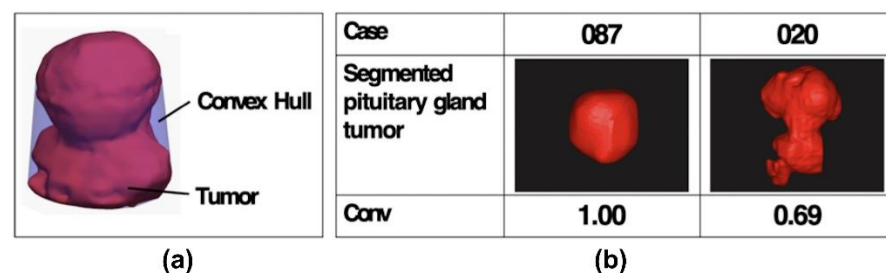


Figure 3. (a) 3D rendering (in purple) of convex hull of a pituitary gland tumor. (b) Examples of pituitary gland tumor with different Conv values: from high (left side) to low (right side).

2.6. Statistical Analysis

We presented continuous data as median, mean \pm standard Deviation (SD). Correlations were assessed using Pearson's or Spearman's method for normally or non-normally distributed data, respectively. The Chi-square test (Fisher's exact test for small numbers) was used for comparisons of categorical variables. We firstly carried out univariate regression logistic models, specific for each variable, to evaluate potential risk or protective prognostic factors related to pituitary tumor surgery. Subsequently, we carried out a step-wise backward regression analysis to select the variables mostly influencing the outcome of interest, i.e., the incomplete tumor resection at follow-up. The significance threshold was fixed at 0.05. Finally, a multivariate regression analysis, including variables that remained significant, was performed. A p -value < 0.05 was considered statistically significant. Statistical analysis was performed using STATA (Statistical software, Version 13—StataCorp LP, College Station, TX, USA).

Parameters included in the analysis were sex, age, tumor type, previous treatment, 2D-based parameters (HD, ICD, Zurich Pituitary Score, Hardy and Wilson grade, Knosp grade), as well as 3D-based indexes (Vol, Area, Spher, Conv). For statistical analysis, the endpoint (tumor removal) parameter was dichotomized as "total" or "incomplete" (including subtotal, partial, or incomplete resection).

3. Results

The series includes 75 patients (41, 54.6%) were male, age: 55.9 ± 16). As reported in Table 1, the majority were non-functioning tumors (58, 77.3%), followed by 9 (12%) PRL tumors, 6 (8%) GH-secreting tumors, and 2 (2.7%) ACTH-secreting ones. Most of the cases were naive (72, 96%) and 3 cases (4%) have undergone previous endoscopic endonasal subtotal resection (in all cases, the second surgery was needed for the progression of the remnant).

Table 1. Patients' pre-operative features. GH = growth hormone; PRL = prolactin; ACTH = adrenocorticotrophic hormone.

		No. of Patients	%
Previous Treatment	none	72	96%
	surgery	3	4%
	radiotherapy	0	0%
Tumor	GH-secreting tumors	6	8%
	PRL-secreting tumors	9	12%
	ACTH-secreting tumors	2	2.7%
	Non-functioning tumors	58	77.3%
Endocrine Functions	none	36	48%
	anterior hypopituitarism	26	34.7%
	Diabetes Insipidus (DI)	1	1.3%
	Acromegaly	6	8%
	Cushing disease	2	2.7%
	HyperPRL (>200 ng/mL)	9	12%
Visual Symptoms	no	35	46.7%
	present	40	53.3%
Ophthalmoplegia	no	69	92%
	present	6	8%

At pre-operative bio-humoral assays, 36 (48%) patients presented a normal pituitary function. In the remaining patients, anterior hypopituitarism was present in 26 (34.7%) cases and isolated Diabetes Insipidus (DI) was evident in 1 (1.3%), already operated on in the past. Acromegaly, i.e., hyper-secretion of GH and insulin-like growth factor 1 (IGF-1), was demonstrated in 6 cases (8%), while a central Cushing disease was confirmed in 2 (2.7%). For elevated levels of serum prolactin (>200 ng/mL) in tumors not responding to

cabergoline treatments, the diagnosis of resistant prolactinoma was suspected in 9 cases (12%). As reported in Table 1, visual disturbances were present pre-operatively in 40 (53.3%) cases, while 6 (8%) patients presented ophthalmoplegia, due to pituitary apoplexy.

As shown in Table 2, most of the tumors were classified as grade 2 according to the Hardy scale (43, 57.3%) and as A or B according to Wilson (respectively, 33 (44%) and 30 (40%)). No CS invasion was suspected in 26 (34.7%) patients (Knosp grade 0), 28 (37.3%) patients presented a low Knosp grade (1 or 2), and 21 (28%) a high grade (3 or 4). The mean maximum horizontal diameter (HD) of the tumor was 23.9 ± 6.3 mm and the mean minimal inter-carotid distance (ICD) was 23.2 ± 3.9 mm; therefore, in the Zurich Pituitary Score system, most of our series were grade 2 (59, 74.7%).

Table 2. Neuroradiological pre-operative features of the patients.

		No. of Patients	%
Hardy	1	6	8%
	2	43	57.4%
	3	16	21.3%
	4	10	13.3%
Wilson	A	33	44%
	B	30	40%
	C	3	4%
	D	1	1.3%
	E	8	10.7%
Knosp	0	26	34.7%
	1	10	13.3%
	2	18	24%
	3	16	21.3%
	4	5	6.7%
Zurich Score	1	5	6.7%
	2	59	78.6%
	3	6	8%
	4	5	6.7%

According to our proposed 3D characterization of the tumor, the mean Vol was 9117 ± 8423 mm³, mean Area was 2352 ± 1571 mm², mean Spher was 0.86 ± 0.08 , and mean Conv was 0.88 ± 0.08 (Table 3). Total tumor removal was achieved in 57 (75%) cases, subtotal in 15 (20%), partial in 1 (1.3%), and incomplete in 2 (2.7%) (Table 3). Surgical complications consisted of 2 (2.7%) post-operative cerebrospinal fluid (CSF) leaks, that have been promptly repaired to avoid meningitis. Other complications were 1 (1.7%) subarachnoidal hemorrhage and 1 (1.7%) surgical field hematoma, which were treated conservatively with the patient's favorable outcome, and 1 (1.7%) transient CN III palsy, which recovered spontaneously after 3 months. Biochemical remission of hyper-secretion was observed in 2 GH adenomas, 5 PRL adenomas, and 1 ACTH adenoma. All patients not presenting a post-operative remission of hyper-secretion started medical therapy, obtaining control of the disease in all cases.

At statistical analysis, the logistic regression demonstrated that Knosp grade and two indexes referring to 3D characterization (i.e., Vol and Conv) were independent significant predictors of the extent of tumor resection (Table 4). Other considered 3D-based factors, including Spher and Area, were not significantly associated with the extent of tumor resection and thus were not included in the final model.

Table 3. Distribution of cavernous sinus (CS) invasion expressed by Knosp grade, tumor volume (Vol), and convexity (Conv) in relation to complete/incomplete surgical resection.

Parameter	Mean \pm SD	Complete Tumor Removal	Incomplete Tumor Removal
Vol	9117 \pm 8423 mm ³	8400 \pm 7792 mm ³	11,365 \pm 10,086 mm ³
Conv	0.88 \pm 0.08	0.91 \pm 0.06	0.80 \pm 0.10
Knosp grade 0	26	24	2
Knosp grade 1	10	8	2
Knosp grade 2	18	14	4
Knosp grade 3	16	11	5
Knosp grade 4	5	0	5

Table 4. Results of logistic regression. The three factors that were independently significantly associated with the extent of tumor resection were Knosp grade, the tumor volume (Vol), and the tumor convexity (Conv). The other potential predictors (Age, Wilson grade, Horizontal Diameter, Sphericity, Area, Zurich Score) were not statistically significant in univariate analysis and they were not included in the final model. For Knosp grade, Odds Ratios referred to Knosp grade 1 (ICD: intercarotid distance, Vol: volume, Conv: convexity, Pre-Treat: previous treatment, Conf.: confidence). The bold data indicating a statistically significant result.

Parameter		z	p	95% Conf. Interval	Odds Ratio	
Sex		−1.43	0.15	0.31	1.72	
Pre-treat		1.07	0.29	0.15	582.45	
Hardy grade		−0.74	0.46	0.19	2.09	
Knosp	2	0.54	0.59	0.45	743.09	18.2
	3	1.06	0.29	0.20	205.21	6.5
	4	1.94	0.05	1.6	1582.61	50.5
Tumor	PRL	0.53	0.59	0.05	158.28	
	ACTH	−0.09	0.93	0.01	177.43	
	NF	−1.52	0.13	0.01	2.06	
ICD		−0.47	0.54	0.68	1.27	0.9
Vol		2.44	0.01	1.01	1.03	1.02
Conv		−2.35	0.02	0.69	0.97	0.8

Knosp grade is significantly correlated with the extent of tumor resection, and the logistic regression permitted to identify that grade 4 is associated with an increased risk of incomplete tumor resection (z score = 1.94, $p = 0.05$).

Among 3D-based parameters, the Vol was found to be directly associated with the risk of incomplete tumor resection (z score 2.44, $p = 0.01$), confirming that for smaller tumors, the chances of complete tumor resection are higher. Particularly, the Odds Ratio was 1.02, meaning that for each increase of 100 mm³ of Vol, the probability of incomplete tumor resection increases by 2%.

Conversely, the Conv was found to be inversely associated with the risk of incomplete tumor resection (z score = −2.35, $p = 0.02$). Indeed, this index increases for more convex tumors and decreases for lesions with many irregularities in the shape, such as hollows or indentations. Therefore, our result demonstrates that adenomas with a reduced Conv, i.e., with a more irregular shape, have an increased chance of incomplete tumor removal.

To investigate the role of these three parameters (Vol, Conv, and Knosp grade) in determining the more favorable outcome, we observed that at univariate logistic regression, only the Conv confirmed its statistical significance (Table 5). Bivariate analysis combining the extent of total tumor resection with Vol and Conv, as well as with Conv and Knosp

grade, shows that, even if both factors are independently involved in the determination of the tumor resection, for tumors with a similar Vol and CS invasion (i.e., Knosp grade), the presence of irregularities in their shape (expressed by a low Conv value) has a major role in the determination of the tumor resection extent (Table 5).

Table 5. The upper section of the table: univariate logistic regression for convexity (Conv) and volume (Vol). The lower section of the table: bivariate analysis showed that for tumors with a similar volume, the presence of irregularities in their shape (expressed by low Conv values) has a major role in the determination of the tumor resection extent. For Knosp grade, Odds Ratios referred to Knosp grade 1.

Parameter	z	p	95% Conf. Interval		Odds Ratio
Conv	−3.87	0.00	0.73	0.90	0.81
Vol	1.61	0.11	1.00	1.01	1.01
Parameter	z	p	95% Conf. Interval		Odds Ratio
Conv	−3.02	0.03	0.73	0.93	0.83
Knosp 2	1.61	0.073	0.80	136.7	10.48
Knosp 3	1.81	0.108	0.66	65.31	6.56
Knosp 4	2.62	0.070	0.86	54.33	6.82

4. Discussion

Our study has shown that parameters derived from 3D modeling and 3D characterization of the tumor, i.e., the tumor volume (Vol) and the presence of shape irregularities expressed by the Conv index, together with CS invasion (particularly for Knosp grade 4) have an independent prognostic role in determining the extent of resection of a pituitary tumor through an EEA.

Although modern technological advancements have permitted to improve the effectiveness of the transsphenoidal route, allowing surgeons to achieve a total removal rate between 50% and 80%, the persistence of remnants remains an issue, exposing the patient to a higher risk of progression/recurrence, persistence of endocrinopathies, or of compressive symptoms [18,23,42–44]. In the pre-surgical phase, it would be relevant to predict the risk of incomplete resection, both for correct patient counseling and to eventually plan post-operative treatments, such as medications for hyper-secretive tumors or radiotherapies. However, it is a common experience in routine clinical settings that some tumors being pre-operatively considered not radically resectable would have a better result than expected, and vice versa. Based on these considerations, multiple studies have recently investigated if pre-operative neuroradiological or clinical factors would be associated with a different extent of tumor removal [14–19,23]. Many parameters have been demonstrated to present a significant prognostic role, such as tumor invasiveness, particularly when the mass extensively grows into the CS, the occurrence of previous surgeries or radiotherapies, the hard or fibrous consistency of the tumor, and its size and diameter [14–17,19,43–49]. Furthermore, a Swiss group has recently proposed a score (Zurich Pituitary Score), which considers the ratio between the ICD and HD of the tumor, and the presence of carotid encasement, to pre-operatively estimate the extent of tumor removal [23].

We have observed that 3D morphological features also have a prominent role in the determination of the tumor extension rate. Indeed, for tumors with a similar Vol and CS invasion degree, the tumor's 3D shape represents a relevant predictive factor. In our study, we have evaluated two 3D-based morphological features of pituitary adenoma, i.e., the Spher and the Conv. With the first, we aimed to consider how much the tumor shape would be similar to that of a sphere, resulting in a round lesion. The second index (Conv) reflects the presence of irregularities more than the Spher, as hollows or indentations, in the 3D tumor shape, identifying lesions with a multi-lobular aspect or an excavated shape. At the statistical analysis, the Conv resulted as the most significantly associated with the risk of an incomplete tumor removal. This can be explained considering that in some cases, as for

ovoidal or flat-geoidal lesions which do not present relevant surgical challenges, the Spher may be low, even if the overall shape is quite regular (i.e., high Conv), and vice versa.

The observation that the resection of tumors invading the CS is challenging dates back to 1955, when Jefferson et al. defined this, and it has remained valid until today [3,17,19,44]. Particularly, considering the predictive roles of the different Knosp grades, we have found that the higher grade (grade 4) was associated with a significantly worse outcome. This can be explained considering that, as shown by Frank et al. [3], and recently confirmed by other studies, only for Knosp 4 grade is it possible to pre-operatively predict the presence of an effective CS invasion by the tumor [3,17,19]. Indeed, in a previous paper of our group, we found that for the grades from 1 to 3B, only 43% of cases were found to be invasive at surgical inspection [19]. However, the Knosp grading system essentially remains an evaluation performed on planar (2D) images. In previous works, the possible benefit of a 3D-based evaluation has been mainly limited to qualitative studies, mostly based on the surgeon's judgment of the tumor morphology at the pre-operative MRI, with consequent limitations to correlate and quantify the role of specific 3D parameters with the tumor resection rate [16,20–24,44].

As was expected, the tumor volume (Vol) also presented an independent prognostic role. Indeed, larger tumors, particularly gigantic ones, are often a challenge for the surgeon. Our observation that Conv has a major prognostic role for tumors with the same Vol confirms the conclusion by Elshazly et al. that giant pituitary tumors can be effectively approached through an EEA, when they present a regular profile [50].

Therefore, we can conclude that it could be extremely useful to analyze the tumor using a 3D approach, since it allows to take into account the presence of a multi-lobular shape or irregularities in its profile, as well as to evaluate possible CS invasion and size via commonly used 2D-based grading systems. This may help the surgeon to plan a correct treatment of a pituitary adenoma. With this study, we would like to emphasize the prognostic role of tumor 3D geometry and morphology, which are usually underestimated in comparison to standard parameters such as size or invasiveness.

As a future perspective of this pilot study, a software tool may be provided to automatically calculate the Spher and Conv parameters starting from reconstructed 3D models of the tumor. The adoption of this tool may be included in the clinical image-based evaluation path of the patient, thus allowing the surgeon to have an additional aid during pre-operative planning for a more accurate decision-making process.

As previously suggested in similar experiences reported for urological surgery [51,52], the proposed 3D-based approach should be considered complementary to the existing staging/scoring system, since the 3D-derived features may provide additional volumetric and morphological parameters that could not be evaluated on 2D images.

The combination of 3D and 2D indexes may be used to define new scoring systems for better characterizing and understanding the complexity of tumors and for predicting complications, thus helping surgeons in planning the surgical approach.

The major limitations of this study are its retrospective nature and the number of cases enrolled. Indeed, although our very strict selection criteria for pre-operative MRI quality have permitted us to collect a homogenous cohort, this has led to a reduction in the sample size. Due to this limitation, the confidence intervals observed in the statistical analysis for some parameters are large. Moreover, due to a possible selection bias, few cases were not naive, and this may have affected the correct interpretation of the prognostic role of this condition. A further bias is the lack of consideration of tumor consistency or histotypes, which have not been included in the analysis because they are not predictable before surgery, and our aim was to assess what pre-operative factors can be effectively adopted to predict the surgical outcome. Finally, we dichotomized the surgical outcome as total or incomplete tumor removal, limiting the possibilities of the statistical analysis, which could be more meaningful with a more complete assessment of surgical outcomes in future prospective larger studies aimed at confirmation of these presented preliminary results. Moreover, we found that this quantitative method of analysis based on 3D virtual

modeling to determine the prognostic role of tumor geometry and morphology could also be extended to other lesions of neurosurgical interest, eventually also considering other 3D-based indexes.

5. Conclusions

In our study, we have observed that 3D morphological features of a pituitary tumor represent a significant independent prognostic factor for total tumor resection. The quantitative analysis and 3D characterization of different pituitary tumors have permitted us to identify that the presence of irregularities, as expressed by a low Conv, has a major negative impact, increasing the risk of incomplete tumor removal. As expected, the other main significant prognostic factor was represented by the Knosp grade, particularly in the case of carotid artery encasement (grade 4) and the tumor size (Vol). Interestingly, for comparable Vol, the more relevant parameter determining the surgical outcome is represented by the 3D irregularity of the tumor shape (Conv).

Based on these results, the 3D geometrical and morphological characterization of the tumor can be considered together with the basic features to achieve accurate pre-operative planning and to guide the surgeon's decision-making process. Further prospective studies are needed to validate these results.

Author Contributions: L.C.: methodology, writing—original draft; M.Z.: conceptualization, writing—original draft; B.B.: software, data curation; N.C.: data curation, writing—reviewing and editing; D.G.: methodology, validation; A.R.: validation, writing—reviewing and editing; D.M.: supervision, writing—reviewing and editing; E.M.: project administration, supervision. All authors have read and agreed to the published version of the manuscript.

Funding: This research received no external funding.

Institutional Review Board Statement: The study was conducted in accordance with the Declaration of Helsinki, and approved by the Institutional inter-hospital Ethical Committee of Bologna City (protocol #CE17143, February 2018).

Informed Consent Statement: Written informed consent was obtained from all subjects involved in the study.

Data Availability Statement: The datasets generated during and/or analyzed during the current study are available from the corresponding author on reasonable request.

Conflicts of Interest: The authors declare no conflict of interest.

References

1. Buchfelder, M.; Schlaffer, S.; Zhao, Y. The optimal surgical techniques for pituitary tumors. *Best Pract. Res. Clin. Endocrinol. Metab.* **2019**, *33*, 101299. [[CrossRef](#)] [[PubMed](#)]
2. Laws, E.R.; Thapar, K. Pituitary surgery. *Endocrinol. Metab. Clin. N. Am.* **1999**, *28*, 119–131. [[CrossRef](#)]
3. Frank, G.; Pasquini, E.; Farneti, G.; Mazzatenta, D.; Sciarretta, V.; Grasso, V.; Fustini, M.F. The Endoscopic versus the Traditional Approach in Pituitary Surgery. *Neuroendocrinology* **2006**, *83*, 240–248. [[CrossRef](#)] [[PubMed](#)]
4. Li, A.; Liu, W.; Cao, P.; Zheng, Y.; Bu, Z.; Zhou, T. Endoscopic Versus Microscopic Transsphenoidal Surgery in the Treatment of Pituitary Adenoma: A Systematic Review and Meta-Analysis. *World Neurosurg.* **2017**, *101*, 236–246. [[CrossRef](#)]
5. Marcus, H.J.; Vercauteren, T.; Ourselin, S.; Dorward, N.L. Intraoperative Ultrasound in Patients Undergoing Transsphenoidal Surgery for Pituitary Adenoma: Systematic Review. *World Neurosurg.* **2017**, *106*, 680–685. [[CrossRef](#)]
6. Pennacchiotti, V.; Garzaro, M.; Grottoli, S.; Pacca, P.; Garbossa, D.; Ducati, A.; Zenga, F. Three-Dimensional Endoscopic Endonasal Approach and Outcomes in Sellar Lesions: A Single-Center Experience of 104 Cases. *World Neurosurg.* **2016**, *89*, 121–125. [[CrossRef](#)]
7. Vasudevan, K.; Saad, H.; Oyesiku, N.M. The Role of Three-Dimensional Endoscopy in Pituitary Adenoma Surgery. *Neurosurg. Clin. N. Am.* **2019**, *30*, 421–432. [[CrossRef](#)]
8. Asioli, S.; Righi, A.; Iommi, M.; Baldovini, C.; Ambrosi, F.; Guaraldi, F.; Zoli, M.; Mazzatenta, D.; Faustini-Fustini, M.; Rucci, P.; et al. Validation of a clinicopathological score for the prediction of post-surgical evolution of pituitary adenoma: Retrospective analysis on 566 patients from a tertiary care centre. *Eur. J. Endocrinol.* **2019**, *180*, 127–134. [[CrossRef](#)]
9. Lopes, M.B.S. The 2017 World Health Organization classification of tumors of the pituitary gland: A summary. *Acta Neuropathol.* **2017**, *134*, 521–535. [[CrossRef](#)]

10. Raverot, G.; Dantony, E.; Beauvy, J.; Vasiljevic, A.; Mikolasek, S.; Borson-Chazot, F.; Jouanneau, E.; Roy, P.; Trouillas, J. Risk of Recurrence in Pituitary Neuroendocrine Tumors: A Prospective Study Using a Five-Tiered Classification. *J. Clin. Endocrinol. Metab.* **2017**, *102*, 3368–3374. [[CrossRef](#)]
11. Trouillas, J.; Roy, P.; Sturm, N.; Dantony, E.; Cortet-Rudelli, C.; Viennet, G.; Bonneville, J.-F.; Assaker, R.; Auger, C.; Brue, T.; et al. A new prognostic clinicopathological classification of pituitary adenomas: A multicentric case–control study of 410 patients with 8 years post-operative follow-up. *Acta Neuropathol.* **2013**, *126*, 123–135. [[CrossRef](#)] [[PubMed](#)]
12. Luomaranta, T.; Raappana, A.; Saarela, V.; Liinamaa, M.J. Factors Affecting the Visual Outcome of Pituitary Adenoma Patients Treated with Endoscopic Transsphenoidal Surgery. *World Neurosurg.* **2017**, *105*, 422–431. [[CrossRef](#)] [[PubMed](#)]
13. Pócož, P.; Kremláček, J.; Česák, T.; Macháčková, M.; Jirásková, N. The Use of Optical Coherence Tomography in Chiasmal Compression. *Czech Slovak Ophthalmol.* **2019**, *75*, 120–127. [[CrossRef](#)] [[PubMed](#)]
14. Kim, J.H.; Lee, J.H.; Lee, J.H.; Hong, A.R.; Kim, Y.J.; Kim, Y.H. Endoscopic Transsphenoidal Surgery Outcomes in 331 Nonfunctioning Pituitary Adenoma Cases After a Single Surgeon Learning Curve. *World Neurosurg.* **2018**, *109*, e409–e416. [[CrossRef](#)] [[PubMed](#)]
15. Knosp, E.; Steiner, E.; Kitz, K.; Matula, C. Pituitary adenomas with invasion of the cavernous sinus space: A magnetic resonance imaging classification compared with surgical findings. *Neurosurgery* **1993**, *33*, 610–618. [[CrossRef](#)]
16. Micko, A.; Oberndorfer, J.; Wening, W.J.; Vila, G.; Höftberger, R.; Wolfsberger, S.; Knosp, E. Challenging Knosp high-grade pituitary adenomas. *J. Neurosurg.* **2019**, *132*, 1739–1746. [[CrossRef](#)]
17. Micko, A.; Woehrer, A.; Wolfsberger, S.; Knosp, E. Invasion of the cavernous sinus space in pituitary adenomas: Endoscopic verification and its correlation with an MRI-based classification. *J. Neurosurg.* **2015**, *122*, 803–811. [[CrossRef](#)]
18. Serra, C.; Burkhardt, J.-K.; Esposito, G.; Bozinov, O.; Pangalu, A.; Valavanis, A.; Holzmann, D.; Schmid, C.; Regli, L. Pituitary surgery and volumetric assessment of extent of resection: A paradigm shift in the use of intraoperative magnetic resonance imaging. *Neurosurg. Focus* **2016**, *40*, E17. [[CrossRef](#)]
19. Zoli, M.; Milanese, L.; Bonfatti, R.; Sturiale, C.; Pasquini, E.; Frank, G.; Mazzatenta, D. Cavernous sinus invasion by pituitary adenomas: Role of endoscopic endonasal surgery. *J. Neurosurg. Sci.* **2016**, *60*, 485–494.
20. Lopez-Garcia, R.; Abarca-Olivas, J.; Monjas-Cánovas, I.; Alfonso, A.P.; Moreno-López, P.; Gras-Albert, J. Endonasal endoscopic surgery in pituitary adenomas: Surgical results in a series of 86 consecutive patients. *Neurocirugia* **2018**, *29*, 161–169. [[CrossRef](#)]
21. Mastorakos, P.; Mehta, G.U.; Chatrath, A.; Moosa, S.; Lopes, M.-B.; Payne, S.C.; Jane, J.A. Tumor to Cerebellar Peduncle T2-Weighted Imaging Intensity Ratio Fails to Predict Pituitary Adenoma Consistency. *J. Neurol. Surg. Part B Skull Base* **2018**, *80*, 252–257. [[CrossRef](#)] [[PubMed](#)]
22. Pappy, A.L.; Savinkina, A.; Bicknese, C.; Neill, S.; Oyesiku, N.M.; Ioachimescu, A.G. Predictive modeling for pituitary adenomas: Single center experience in 501 consecutive patients. *Pituitary* **2019**, *22*, 520–531. [[CrossRef](#)] [[PubMed](#)]
23. Serra, C.; Staartjes, V.E.; Maldaner, N.; Muscas, G.; Akeret, K.; Holzmann, D.; Soyka, M.B.; Schmid, C.; Regli, L. Predicting extent of resection in transsphenoidal surgery for pituitary adenoma. *Acta Neurochir.* **2018**, *160*, 2255–2262. [[CrossRef](#)] [[PubMed](#)]
24. Do, H.; Kshetry, V.R.; Siu, A.; Belinsky, I.; Farrell, C.J.; Nyquist, G.; Rosen, M.; Evans, J.J. Extent of Resection, Visual, and Endocrinologic Outcomes for Endoscopic Endonasal Surgery for Recurrent Pituitary Adenomas. *World Neurosurg.* **2017**, *102*, 35–41. [[CrossRef](#)]
25. Rana, M.; Essig, H.; Eckardt, A.M.; Tavassol, F.; Ruecker, M.; Schramm, A.; Gellrich, N.-C. Advances and Innovations in Computer-Assisted Head and Neck Oncologic Surgery. *J. Craniofacial Surg.* **2012**, *23*, 272–278. [[CrossRef](#)]
26. Pellegrino, G.; Ferri, A.; Cercenelli, L.; Marcelli, E.; Marchetti, C.; Tarsitano, A.; Ciocca, L. 3D planning of ear prosthesis and navigated flapless surgery for craniofacial implants: A pilot study. *J. Stomatol. Oral Maxillofac. Surg.* **2021**, *122*, 391–396. [[CrossRef](#)]
27. Checcucci, E.; Amparore, D.; Fiori, C.; Manfredi, M.; Ivano, M.; Di Dio, M.; Niculescu, G.; Piramide, F.; Cattaneo, G.; Piazzolla, P.; et al. 3D imaging applications for robotic urologic surgery: An ESUT YAUWP review. *World J. Urol.* **2019**, *38*, 869–881. [[CrossRef](#)]
28. Bianchi, L.; Barbaresi, U.; Cercenelli, L.; Bortolani, B.; Gaudiano, C.; Chessa, F.; Angiolini, A.; Lodi, S.; Porreca, A.; Bianchi, F.M.; et al. The Impact of 3D Digital Reconstruction on the Surgical Planning of Partial Nephrectomy: A Case-control Study. Still Time for a Novel Surgical Trend? *Clin. Genitourin. Cancer* **2020**, *18*, e669–e678. [[CrossRef](#)]
29. Bianchi, L.; Schiavina, R.; Bortolani, B.; Cercenelli, L.; Gaudiano, C.; Carpani, G.; Rustici, A.; Droghetti, M.; Mottaran, A.; Boschi, S.; et al. Interpreting nephrometry scores with three-dimensional virtual modelling for better planning of robotic partial nephrectomy and predicting complications. *Urol. Oncol. Semin. Orig. Investig.* **2021**, *39*, 836.e1–836.e9. [[CrossRef](#)]
30. Panesar, S.S.; Magnetta, M.; Mukherjee, D.; Abhinav, K.; Branstetter, B.F.; Gardner, P.A.; Iv, M.; Fernandez-Miranda, J.C. Patient-specific 3-dimensionally printed models for neurosurgical planning and education. *Neurosurg. Focus* **2019**, *47*, E12. [[CrossRef](#)]
31. Tarsitano, A.; Ricotta, F.; Cercenelli, L.; Bortolani, B.; Battaglia, S.; Lucchi, E.; Marchetti, C.; Marcelli, E. Pretreatment tumor volume and tumor sphericity as prognostic factors in patients with oral cavity squamous cell carcinoma. *J. Cranio-Maxillofac. Surg.* **2019**, *47*, 510–515. [[CrossRef](#)] [[PubMed](#)]
32. Casanueva, F.F.; Barkan, A.L.; Buchfelder, M.; Klibanski, A.; Laws, E.R.; Loeffler, J.S.; Melmed, S.; Mortini, P.; Wass, J.; Giustina, A. Criteria for the definition of Pituitary Tumor Centers of Excellence (PTCOE): A Pituitary Society Statement. *Pituitary* **2017**, *20*, 489–498. [[CrossRef](#)] [[PubMed](#)]

33. Faustini-Fustini, M.; Pasquini, E.; Zoli, M.; Mazzatenta, D.; Frank, G. Pituitary Centers of Excellence. *Neurosurgery* **2013**, *73*, E557. [[CrossRef](#)] [[PubMed](#)]
34. Barazi, S.A.; Pasquini, E.; D'Urso, P.I.; Zoli, M.; Mazzatenta, D.; Sciarretta, V.; Frank, G. Extended endoscopic transplanum-transsterculum approach for pituitary adenomas. *Br. J. Neurosurg.* **2012**, *27*, 374–382. [[CrossRef](#)] [[PubMed](#)]
35. Badiali, G.; Marcelli, E.; Bortolani, B.; Marchetti, C.; Cercenelli, L. An average three-dimensional virtual human skull for a template-assisted maxillofacial surgery. *Int. J. Artif. Organs* **2019**, *42*, 566–574. [[CrossRef](#)]
36. Battaglia, S.; Ricotta, F.; Maiolo, V.; Savastio, G.; Contedini, F.; Cipriani, R.; Bortolani, B.; Cercenelli, L.; Marcelli, E.; Marchetti, C.; et al. Computer-assisted surgery for reconstruction of complex mandibular defects using osteomyocutaneous microvascular fibular free flaps: Use of a skin paddle-outlining guide for soft-tissue reconstruction. A technical report. *J. Cranio-Maxillofac. Surg.* **2018**, *47*, 293–299. [[CrossRef](#)]
37. Bianchi, L.; Schiavina, R.; Barbaresi, U.; Angiolini, A.; Pultrone, C.V.; Manferrari, F.; Bortolani, B.; Cercenelli, L.; Borghesi, M.; Chessa, F.; et al. 3D Reconstruction and physical renal model to improve percutaneous puncture during PNL. *Int. Braz. J. Urol.* **2019**, *45*, 1281–1282. [[CrossRef](#)]
38. Ricotta, F.; Cercenelli, L.; Battaglia, S.; Bortolani, B.; Savastio, G.; Marcelli, E.; Marchetti, C.; Tarsitano, A. Navigation-guided resection of maxillary tumors: Can a new volumetric virtual planning method improve outcomes in terms of control of resection margins? *J. Cranio-Maxillofac. Surg.* **2018**, *46*, 2240–2247. [[CrossRef](#)]
39. Schiavina, R.; Bianchi, L.; Borghesi, M.; Chessa, F.; Cercenelli, L.; Marcelli, E.; Brunocilla, A. Three-dimensional digital reconstruction of renal model to guide preoperative planning of robot-assisted partial nephrectomy. *Int. J. Urol.* **2019**, *26*, 931–932. [[CrossRef](#)]
40. Wadell, H. Volume, Shape, and Roundness of Quartz Particles. *J. Geol.* **1935**, *43*, 250–280. [[CrossRef](#)]
41. Dhar, S.; Tremmel, M.; Mocco, J.; Kim, M.; Yamamoto, J.; Siddiqui, A.H.; Hopkins, L.N.; Meng, H. Morphology parameters for intracranial aneurysm rupture risk assessment. *Neurosurgery* **2008**, *63*, 185–197. [[CrossRef](#)] [[PubMed](#)]
42. Dallapiazza, R.F.; Grober, Y.; Starke, R.M.; Laws, E.R.; Jane, J.A. Long-term Results of Endonasal Endoscopic Transsphenoidal Resection of Nonfunctioning Pituitary Macroadenomas. *Neurosurgery* **2014**, *76*, 42–53. [[CrossRef](#)] [[PubMed](#)]
43. Dehdashti, A.R.; Ganna, A.; Karabatsou, K.; Gentili, F. Pure endoscopic endonasal approach for pituitary adenomas: Early surgical results in 200 patients and comparison with previous micro-surgical series. *Neurosurgery* **2008**, *62*, 1006–1017. [[CrossRef](#)] [[PubMed](#)]
44. Dhandapani, S.; Singh, H.; Negm, H.M.; Cohen, S.; Anand, V.K.; Schwartz, T.H. Cavernous Sinus Invasion in Pituitary Adenomas: Systematic Review and Pooled Data Meta-Analysis of Radiologic Criteria and Comparison of Endoscopic and Microscopic Surgery. *World Neurosurg.* **2016**, *96*, 36–46. [[CrossRef](#)]
45. Nishioka, H.; Hara, T.; Nagata, Y.; Fukuhara, N.; Yamaguchi-Okada, M.; Yamada, S. Inherent Tumor Characteristics That Limit Effective and Safe Resection of Giant Nonfunctioning Pituitary Adenomas. *World Neurosurg.* **2017**, *106*, 645–652. [[CrossRef](#)]
46. Juraschka, K.; Khan, O.H.; Godoy, B.L.; Monsalves, E.; Kilian, A.; Krischek, B.; Ghare, A.; Vescan, A.; Gentili, F.; Zadeh, G. Endoscopic endonasal transsphenoidal approach to large and giant pituitary adenomas: Institutional experience and predictors of extent of resection. *J. Neurosurg.* **2014**, *121*, 75–83. [[CrossRef](#)]
47. Sylvester, P.T.; Evans, J.A.; Zipfel, G.J.; Chole, R.A.; Uppaluri, R.; Haughey, B.H.; Getz, A.E.; Silverstein, J.; Rich, K.M.; Kim, A.H.; et al. Combined high-field intraoperative magnetic resonance imaging and endoscopy increase extent of resection and progression-free survival for pituitary adenomas. *Pituitary* **2015**, *18*, 72–85. [[CrossRef](#)]
48. Hofstetter, C.P.; Nanaszko, M.J.; Mubita, L.L.; Tsiouris, J.; Anand, V.K.; Schwartz, T.H. Volumetric classification of pituitary macroadenomas predicts outcome and morbidity following endoscopic endonasal transsphenoidal surgery. *Pituitary* **2011**, *15*, 450–463. [[CrossRef](#)]
49. Little, A.S.; Chicoine, M.R.; Kelly, D.F.; Sarris, C.E.; Mooney, M.A.; White, W.L.; Gardner, P.A.; Fernandez-Miranda, J.C.; Barkhoudarian, G.; Chandler, J.P.; et al. Evaluation of Surgical Resection Goal and Its Relationship to Extent of Resection and Patient Outcomes in a Multicenter Prospective Study of Patients With Surgically Treated, Nonfunctioning Pituitary Adenomas: A Case Series. *Oper. Neurosurg.* **2019**, *18*, 26–33. [[CrossRef](#)]
50. Elshazly, K.; Kshetry, V.R.; Farrell, C.J.; Nyquist, G.; Rosen, M.; Evans, J.J. Clinical Outcomes After Endoscopic Endonasal Resection of Giant Pituitary Adenomas. *World Neurosurg.* **2018**, *114*, e447–e456. [[CrossRef](#)]
51. Bianchi, L.; Schiavina, R.; Bortolani, B.; Cercenelli, L.; Gaudiano, C.; Mottaran, A.; Droghetti, M.; Chessa, F.; Boschi, S.; Molinaroli, E.; et al. Novel Volumetric and Morphological Parameters Derived from Three-dimensional Virtual Modeling to Improve Comprehension of Tumor's Anatomy in Patients with Renal Cancer. *Eur. Urol. Focus* **2021**. *online ahead of print*. [[CrossRef](#)] [[PubMed](#)]
52. Porpiglia, F.; Amparore, D.; Checucci, E.; Manfredi, M.; Stura, I.; Migliaretti, G.; Autorino, R.; Ficarra, V.; Fiori, C. Three-dimensional virtual imaging of renal tumours: A new tool to improve the accuracy of nephrometry scores. *Br. J. Urol.* **2019**, *124*, 945–954. [[CrossRef](#)] [[PubMed](#)]